Low Temperature Scanning Force Microscopy of the Si(111)-(7 × 7) Surface

M. A. Lantz,[1] H. J. Hug,[1] P. J. A. van Schendel,[1] R. Hoffmann,[1] S. Martin,[1] A. Baratoff,[1]
A. Abdurixit,[1] H.-J. Güntherodt,[1] and Ch. Gerber[2]

[1]*Institute of Physics, University of Basel, Klingelbergstrasse 82, CH-4056 Basel, Switzerland*
[2]*IBM Research Division, Zürich Research Laboratory, Säumerstrasse 4, CH-8803 Rüschlikon, Switzerland*
(Received 1 December 1999)

A low temperature scanning force microscope (SFM) operating in a dynamic mode in ultrahigh vacuum was used to study the Si(111)-(7 × 7) surface at 7.2 K. Not only the twelve adatoms but also the six rest atoms of the unit cell are clearly resolved for the first time with SFM. In addition, the first measurements of the short range chemical bonding forces above specific atomic sites are presented. The data are in good agreement with first principles computations and indicate that the nearest atoms in the tip and sample relax significantly when the tip is within a few Å of the surface.

PACS numbers: 61.16.Ch, 07.79.–v, 34.20.Cf

Scanning force microscopy (SFM) is a well established tool for studying the topography of both conducting and insulating surfaces on the nanometer scale. The versatility of the technique has led to rapid growth in its application, which has in turn resulted in progress in the attainable resolution. A significant step was made in 1995 with the resolution of adatoms on the Si(111)-(7 × 7) surface using dynamic mode SFM operating in ultrahigh vacuum (UHV) [1,2]. In view of the characteristic features within its unit cell (faulted half, corner hole, adatoms, and rest atoms) this surface is well suited as a benchmark for SFM. Despite impressive advances in SFM resolution, the mechanisms underlying true atomic resolution are still not well understood. For example, Uchihashi *et al.* [3] claimed that optimum resolution on the Si(111)-(7 × 7) surface is achieved in a soft intermittent contact mode, whereas Lüthi *et al.* [4] obtained images showing adatoms and point defects in the noncontact regime where the measured frequency shift steeply decreases upon approach. Furthermore, the contrast demonstrated often varies between reports. For example, Nakagiri *et al.* [5] and Uchihashi *et al.* [3], using a Si tip, observed a height difference between the two halves of the unit cell as well as reporting the corner adatoms as appearing higher than the center adatoms. In contrast, Erlandsson *et al.* [6], using a tungsten tip, reported the center adatoms as higher than the corner adatoms. Atomic scale SFM contrast on the Si(111)-(7 × 7) surface has been attributed to a partially filled dangling bond on the tip apex interacting with nearby dangling bonds on the surface adatoms. This interpretation was strongly reinforced by the work of Perez *et al.* [7] who used density functional theory (DFT) calculations to simulate a model silicon tip interacting with a Si(111)-(5 × 5) surface. However, in contrast to previous experimental reports where only the adatoms have been imaged, the work of Perez *et al.* indicates that it should also be possible to image the rest atoms on the Si(111)-(7 × 7) surface.

In this Letter we report true atomic resolution images of the Si(111)-(7 × 7) surface obtained by SFM at 7.2 K. SFM operation at low temperature reduces the thermal vibrations in the cantilever resulting in improved sensitivity [8]. In addition, thermal drift is significantly reduced allowing more accurate positioning and slower scan speeds. This has permitted us to obtain images of a quality comparable to scanning tunneling microscopy and to observe both the adatoms and the rest atoms on the Si(111)-(7 × 7) surface. More importantly, we have performed constant height scans at a series of tip-sample distances and used the data to extract the first measurements of the interaction potential above specific sites.

The experiments were performed using a homebuilt low temperature UHV SFM [8], and a p-type silicon sample with a resistivity of 3–6 Ω cm. After transfer into the UHV system, a Si(111)-(7 × 7) reconstructed surface was prepared by direct current heating. Imaging was performed using a commercial silicon cantilever. The fundamental resonance frequency f_0 and Q of the cantilever, measured at 7.2 K, were 155 719.3 Hz and 370 000, respectively. The spring constant ($k = 28.6$ N/m) was calculated from the resonance frequency and the measured length and width of the cantilever [9]. After transfer into the UHV system, the cantilever was heated to 130 °C for two hours to remove absorbed contaminant layers. No additional cleaning procedures were performed, and as such we assume that the tip was initially covered with a thin native oxide layer.

Imaging was performed in the dynamic mode using a frequency modulation (FM) technique in which the cantilever is driven at its resonant frequency at constant oscillation amplitude [10]. For all the experiments described here, an amplitude of 5 nm was used and both the tip and sample were grounded. Two imaging modes were used: *topographic* and *constant height*. In the *topographic* mode, the minimum tip-sample spacing is controlled by a feedback loop in order to maintain a constant frequency shift. The displacement of the sample is recorded and used to produce a topographic map of the surface. In the *constant height* mode, a plane parallel to the surface (determined

 0031-9007/00/84(12)/2642(4)$15.00

in the topographic mode) is scanned without displacement feedback. The resulting frequency shift is recorded and used to produce an image of the surface.

Upon first imaging the sample, weak atomic scale contrast was observed. However, with continued imaging, abrupt changes in contrast were observed. These changes probably resulted from the transfer of a few silicon atoms from the surface to the apex of the tip. After several such events, imaging became stable, and reproducible, high quality images of the surface were obtained. Figure 1(a) shows a 10×7 nm^2 image obtained in the topographic mode at a frequency shift of -27 Hz and a scanning speed of 10 nm/s. In this image, the six adatoms in each half-unit cell are clearly resolved as pronounced maxima, consistent with strong attraction to these sites. In addition, small differences in height between inequivalent adatom sites and weak maxima above the three rest atoms can be detected. These details can be more clearly observed in line sections or by taking smaller area images at larger negative frequency shifts and at slower scan speeds. Figure 1(b) shows a 5×5 nm^2 topographic image obtained at a frequency shift of -31 Hz and a scanning speed of 0.63 nm/s. Under these conditions, the rest atoms are clearly observed. From the two line sections shown in Figs. 1(d) and 1(e), it is clear that we observe additional local maxima and not saddle points. The observation of these additional maxima cannot be due to a double-tip effect as this would manifest itself as six additional maxima per unit cell, whereas we observe only three rest atoms per half unit cell. It is also clear from the position of the additional maxima that their observation is not an artifact resulting from the tip scanning between two adatoms. Figure 1(c) shows top and side views of the dimer-adatom-stacking fault (DAS) model [11] of the Si(111)-(7×7) surface. For reference, the unit cell is outlined with a grey line in Figs. 1(b) and 1(c). Figure 1(d) shows a line section along the long diagonal of the unit cell from the image in Fig. 1(b). Comparison with the DAS model shows good agreement except for a slight shift in the position of the rest atoms towards the right in comparison to the model. This shift is probably due to the finite angle (12°) at which the cantilever is mounted with respect to the sample. This can lead to a systematic distortion because the force normal to the surface of the cantilever is measured rather than the force perpendicular to the sample surface [12].

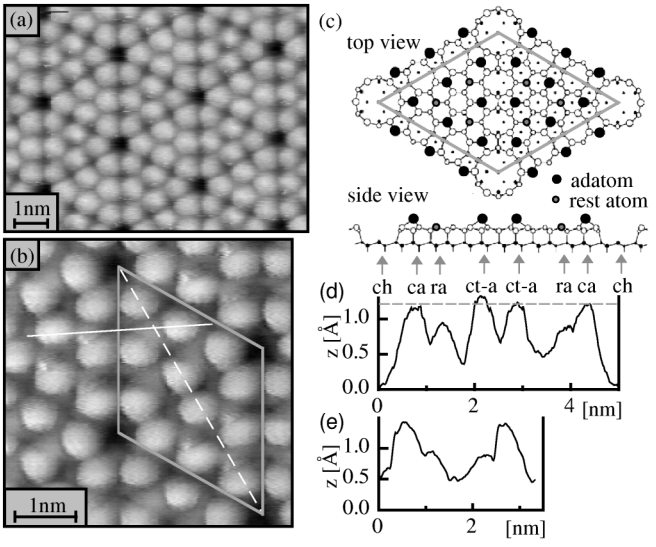

FIG. 1. (a) 10×7 nm^2 image obtained in the topographic mode. (b) 5×5 nm^2 topographic image. (c) DAS model of the Si(111)-(7×7) surface. (d),(e) Line sections taken along the solid and dashed white lines, respectively, in (b). The dashed grey line is a guide for the eye to highlight height differences. ch, ca, ra, and ct-a denote the corner hole, corner adatom, rest atom, and center adatom, respectively.

The overall magnitude of the corrugation observed in the images shown in Fig. 1 is somewhat smaller than that obtained by Uchihashi *et al.* [3] and slightly larger than that observed by others [4,6]. All of these measured corrugations are at least a factor of 2 smaller than the corrugation at constant force that can be inferred from the force-distance characteristics due to chemical forces, computed by Perez *et al.* [7]. To understand this, we note that the frequency shift results from both chemical and van der Waals forces. The reduced measured corrugation can then be attributed to the contribution of the distance dependent, but essentially site independent van der Waals attraction which comes from an effective volume containing many atoms, even at the relevant minimum tip-sample spacings. For example, when the apex of the tip is above a rest atom, the average distance between tip and sample is smaller compared to when the tip is above an adatom. This decrease in the average distance gives rise to an increase in the van der Waals force which results in a decrease in the apparent height of the rest atoms; i.e., the relative contribution of the van der Waals force to the frequency shift is larger above the rest atoms than above the adatoms. This highlights the important point that the microscopic tip shape has a strong influence on the corrugation observed at constant frequency shift. If the tip is not sharp, such that the van der Waals force is large compared to the chemical contribution to the frequency shift, the contrast above the rest atoms will be very small.

It is interesting to compare the measured height differences to the theoretical positions of the atoms, calculated in the absence of a tip. The calculated height differences between the adatoms are very small, less then 0.1 Å, with the faulted corner adatoms highest [13]. In contrast, experimentally we find that the center adatoms in one-half of the unit cell are imaged highest and that the relative height differences depend on the imaging conditions. Taking the highest center adatoms as a reference, we find that at a frequency shift of -31 Hz, the corner adatoms in the same half of the unit cell are imaged approximately 0.17 Å lower, and in the other half of the unit cell, both types of adatoms are imaged at approximately the same

height, 0.10 Å lower. At smaller frequency shifts we find smaller relative height differences. For the case of the rest atoms, we also find that the measured height depends on the frequency shift. At a frequency shift of -31 Hz, the rest atoms are imaged at approximately 0.40 Å below the highest adatom. This is much smaller than the theoretically calculated height difference of 1.0 Å. Clearly, the experimental height contrast is not due to purely structural effects and therefore the observed differences are likely induced by variations in the interaction potential above different atomic sites. This interpretation is supported by the work of Perez *et al.* [7] who found such differences on the Si(111)-(5 × 5) surface [which exhibits the characteristic features of the Si(111)-(7 × 7) surface]. These site specific differences in the interaction potentials are related to differences in the electronic charge distribution. A direct comparison of the differences between inequivalent adatoms is therefore not straightforward because there are small but important differences in the electronic charge distribution on the 5 × 5 and 7 × 7 surfaces [14].

In order to gain a better understanding of the mechanisms which give rise to the observed atomic contrast, we have recorded constant height images of the surface at progressively smaller tip-sample spacings. In Fig. 2 we have plotted line sections from a series of constant height images taken at progressively smaller tip-sample spacings. The line sections were taken at the same location, namely, through one-half of the unit cell, along the long diagonal. To facilitate comparison with other experiments, both the frequency shift, Δf, and the normalized frequency shift γ are displayed ($\gamma = \Delta f k A_0^{3/2}/f_0$) [15]. Here k is the spring constant of the cantilever, A_0 is the oscillation amplitude, and f_0 is the unperturbed resonance frequency. At the largest tip-sample spacing (z_0 in Fig. 2), the average frequency shift was -22 Hz and the image showed no recognizable atomic scale contrast. We therefore assume that at this distance the frequency shift is due predominantly to the van der Waals interaction. In the subsequent scan, performed with the sample displaced only 0.22 Å towards the cantilever, the adatoms were clearly resolved. At this spacing, the frequency shift above the corner hole decreased by only an additional -2 Hz, whereas above the adatoms we observe an additional frequency shift of approximately -20 Hz. As the tip-sample spacing was reduced further, the frequency shift above the corner hole still changed slowly while the frequency shift above the adatoms changed rapidly. A similar rapid variation in frequency shift has been previously reported by Uchihashi *et al.* [3]; however, in previous room temperature work [1–6], force spectroscopy of specific atomic positions was not possible. When the tip sample spacing was reduced by 0.64 Å, we began to detect the rest atoms. It is also worth noting that subtle differences between the frequency shift above the corner and center adatoms are observed, as expected. At the largest frequency shift measured, the peak attractive force acting on the tip is estimated to be on the order of a few nanonewtons. In a hypothetical static constant height measurement, such a force would give rise to a significant deflection of the cantilever and result in a modulation of the tip-sample spacing as the cantilever is scanned above the surface. This is not the case in the large oscillation amplitude dynamic mode. The very small relative frequency shift (<200 Hz compared to a free resonance frequency of 156 kHz) indicates that the total potential acting on the tip differs only slightly from the harmonic potential. A detailed calculation shows that the change in the tip-sample distance due to the force acting on the tip is less than a picometer for the measurements presented here.

Using the data presented in Fig. 2, we can determine the range of the tip-sample interaction above different sites and compare it to theoretical interaction potentials. In Fig. 3, the frequency shift above the corner hole and center adatom are plotted as a function of the sample displacement. A striking feature is the relatively large change in the frequency shift above the adatoms resulting from a change in the sample displacement of less than 1 Å. The perturbation theory for the frequency shift Δf [15] implies that $\Delta f(d)$, normalized to -1 and plotted versus the minimum tip-sample spacing, d, lies between the corresponding curves for the tip-sample interaction energy and force. Hence, the position of the maximum in the slope of the frequency shift curve is a measure of the range of the attractive interaction. Note that at room temperature, the thermal displacement noise of the cantilever would typically be comparable to the width of the attractive part of

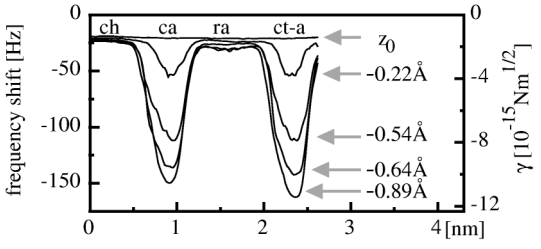

FIG. 2. Line sections taken from a series of constant height scans made at progressively smaller tip-sample spacings.

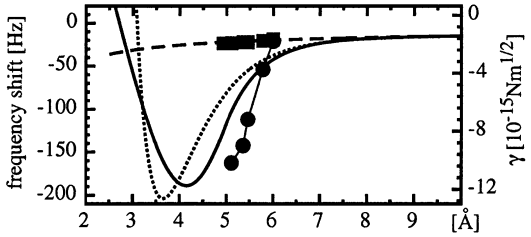

FIG. 3. Frequency shift measured above a corner hole (squares) and center adatom (circles) plotted versus sample displacement. The dashed, dotted, and solid lines show frequency shifts calculated from theoretical tip-sample interaction forces (see text). For the interaction shown by the solid line, the maximum attractive force is -2.66 nN.

the short range interaction measured here. It is therefore not surprising that it is difficult to maintain stable imaging conditions in room temperature experiments. Further, we note that the thermal noise will have an averaging effect, resulting in an apparent potential with an artificially broader range. To make a direct comparison with theoretical interaction potentials, we used the perturbation formula first derived by Giessibl [15] to calculate the frequency shift Δf due to an interaction force F_{int}:

$$\Delta f(d) = \frac{-f_0^2}{kA_0^2} \int_0^{1/f_0} F_{\text{int}}[d + A_0 + z(t)]z(t)\, dt\,, \quad (1)$$

where $z(t) = A_0 \cos(2\pi f_0 t)$ and d, k, A_0, and f_0 are as defined above. At the small tip sample distances studied here, we expect that the interaction force results from a long range van der Waals interaction and a short range chemical interaction. In order to separate these two effects, we assume that the frequency shift observed above the corner hole is due to only the van der Waals interaction. For a conical tip and a flat surface the corresponding force is $F_{\text{vdW}} = -A_H 4 \tan^2(\alpha/2)/6\pi d$, where A_H is the Hamaker constant of silicon and α is the full cone angle of the tip [15]. A reasonable fit to the data is obtained with $A_H \tan^2(\alpha/2) = 0.19aJ$, as shown by the dashed line in Fig. 3. Experimentally we measure the sample displacement but do not know the absolute tip-sample distance. We have therefore plotted the experimental data by choosing the absolute tip-sample distance to be consistent with the calculated frequency shifts.

To model the interaction above the adatoms, we calculated the frequency shift due to the sum of the van der Waals force given above and the derivative of a Morse potential. The total frequency shift is shown by the dotted line in Fig. 3. For the Morse potential we have used the fit by Perez *et al.* [7] to their calculated interaction between a silicon tip and an adatom in the unfaulted half of the unit cell, plotted as a function of the distance between the adatom and the closest atom in the tip. Comparing the theoretical and experimental frequency shifts we note that the magnitudes are in reasonable agreement but, surprisingly, the experimental data change much more rapidly than the calculated frequency shift. We believe that this disparity results from relaxation effects in the tip and sample. Experimentally we measure the displacement of the sample; however, as the tip-sample spacing is reduced, the attractive force due to the highly localized chemical interaction between the closest atoms of the tip and sample results in additional displacements of these two atoms towards each other [7]. Thus, the actual change in distance between the closest atoms is larger than the experimentally measured sample displacement, making the attractive part of the experimental potential appear steeper. To account for these relaxation effects, we have fit the force versus sample displacement curve reported by Perez *et al.* [7] and used it to recalculate the total frequency shift (solid line in Fig. 3). Both the slope and the magnitude of the frequency shift are in better agreement with our experimental data; however, the calculated slope is still smaller. We interpret this as an indication that the experimental relaxation effects are larger than those calculated by Perez *et al.*, which is not surprising because their model tip was a cluster containing only ten silicon atoms.

In conclusion, we have reported the first SFM images of the rest atoms and the first site specific measurements of the short range interaction between a silicon tip and the Si(111)-(7 × 7) surface. We found that the chemical interaction is large, is very short range, and changes dramatically with lateral position. This information is not accessible via images acquired in the constant frequency mode. Instead, a series of images of the site dependent frequency shift at closely spaced constant heights or a series of frequency distance characteristics must be used. Such demanding measurements are possible only because of the very small thermal drift and high stability of our low temperature SFM.

We are grateful to C. Loppacher for helpful discussions. This work was partially supported by the Swiss priority program NFP 36.

[1] F. J. Giessibl, Science **267**, 68 (1995).
[2] S. Kitamura and M. Iwatsuki, Jpn. J. Appl. Phys. **34**, 145 (1995).
[3] T. Uchihashi *et al.*, Phys. Rev. B **56**, 9834 (1997).
[4] R. Lüthi *et al.*, Surf. Rev. Lett. **4**, 1025 (1997).
[5] N. Nakagiri, M. Suzuki, K. Okiguchi, and H. Sugimura, Surf. Sci. **373**, L329 (1997).
[6] R. Erlandsson, L. Olsson, and P. Martensson, Phys. Rev. B **54**, R8309 (1996).
[7] R. Perez, I. Stich, M. C. Payne, and K. Terakura, Phys. Rev. B **58**, 10 835 (1998).
[8] H. J. Hug *et al.*, Rev. Sci. Instrum. **70**, 3625 (1999).
[9] U. Rabe, K. Janser, and W. Arnold, Rev. Sci. Instrum. **67**, 3281 (1996).
[10] C. Loppacher *et al.*, Appl. Phys. A **66**, 215 (1998).
[11] K. Takayanagi, Y. Tanishiro, M. Takahashi, and S. Takahashi, J. Vac. Sci. Technol. **3**, 1502 (1985).
[12] D. Rugar *et al.*, J. Appl. Phys. **68**, 1169 (1990).
[13] K. D. Brommer, M. Needles, B. E. Larson, and J. D. Joannopoulos, Phys. Rev. Lett. **68**, 1355 (1992).
[14] I. Stich, M. C. Payne, R. D. King-Smith, and J.-S. Lin, Phys. Rev. Lett. **68**, 1351 (1992).
[15] F. J. Giessibl, Phys. Rev. B **56**, 16 010 (1997).